Journal of ELECTRICAL ENGINEERING, VOL. 57, NO. 4, 2006, 193–199

PARK MODEL OF SQUIRREL CAGE INDUCTION MACHINE INCLUDING SPACE HARMONICS EFFECTS

Mohamed Boucherma — Mohamed Yazid Kaikaa — Abdelmalek Khezzar *

An accurate and simpler approach for modelling and simulating the dynamic behavior of squirrel cage induction machines is presented here. The model is based on multiple coupled circuits and takes into account the geometry and winding layout of the machine. All inductances are derived by means of the winding function approach (WFA) and are integrated with the decomposition into their Fourier series. An important issue in such effort is the modelling of the induction motor including rotor slot harmonics (RSH) under symmetrical and asymmetrical conditions, with minimum computational complexity. Simulations results have shown excellent match with theoretically predicted RSH components.

K e y w o r d s: induction machine, Park model, space harmonics, winding function, diagnostics

1 INTRODUCTION

For past 30 years, the dynamic behaviour of induction machine has received a considerable attention in most researched works. However, the majority of models are based on the simple idealist machine without tacking into account the physical layout of the stator and rotor windings. For example, the conventional Park (dq) model and the development of its current, torque and power relationships are based on the assumptions that the rotating mmf produced by stator winding excitation is sinusoidally distributed in space and that the rotor mmf due to the slip frequency induced currents is similarly distributed. It is apparent that these models are not suitable for diagnosis and/or sensorless speed estimation by investigating the rotor slot harmonics (RSH). Therefore, there is a real need to derive an accurate model which can take into account the effect of the field harmonics both in time and in space.

There are several papers devoted to this problem; in the papers [1, 2], the space harmonics are taking into account by means of the winding function approach (WFA). The model developed is based directly on the geometry of the induction machine and the physical layout of all windings. This model has been next extended to monitor some mechanical and electrical defaults: inter-turn short circuits in the stator windings [3,4], rotor eccentricity [5,6] and to estimate the rotor speed for the control purpose [7,8,9].

In this paper, an alternative way for formulating the suitable model is suggested, using the decomposition into Fourier series of the mutual inductance matrix and the presentation of the induction motor in Park frame. It is found that an accurate motor simulation can be achieved with the proposed method, in addition, this speeds up significantly the computer simulation time, and makes the process monitoring more reliable. The new model can be extended to the solution of a wide variety of fault and predict the squirrel induction motor response in transient as well as in steady-state modes of operation. The detailed depiction of the procedure needed to implement such an accurate model with simulation results is the subject of this paper

2 THEORETICAL BACKGROUND: ROTOR SLOT HARMONICS

The air gap field of an induction motor fed by a sinusoidal voltage supply waveform comprises a wide range of different space harmonics. The following analysis assumes that these air-gap flux harmonics are a result of the interaction of air-gap permeance and harmonic magnetomotive force (MMF) waves. Only harmonics due to slotting are considered here (rotor slot harmonics).

It has been shown that the rotor slot harmonics (RSH) are generated in the stator line current for healthy machine at frequencies given by [3,5]:

$$f_{sh} = \left(\frac{\lambda N_r}{p} (1 - s) \pm 1 \right) f \tag{1}$$

Note that only RSH who's their order belongs to the following set can be detected [9,10]:

$$G = \left\{ (6k \pm 1)_{k=1,2,3} \cup \left(\frac{\lambda N_r}{p} \pm 1 \right)_{\lambda=1,2,3,\cdots} \right\} \tag{2}$$

For a rotor with asymmetry (broken bar, end-ring fault or eccentricity) Thomson and al. have shown that the rotor slot harmonic frequencies are [11]:

$$f_{hk} = \left(\lambda \frac{N_r}{p} (1 - s) \pm 1 \pm 2ks \right) f_s \tag{3}$$

where: p— is the number of pole pairs and S is the slip.; f_S — is the fundamental supply frequency; N_r — is the number of rotor slot (bars0; λ — is a positive integer.

Electrical Laboratory of Constantine (LEC), Department of Electrical Engineering, Mentouri University–Constantine, 25000 Constantine, Algeria

ISSN 1335-3632

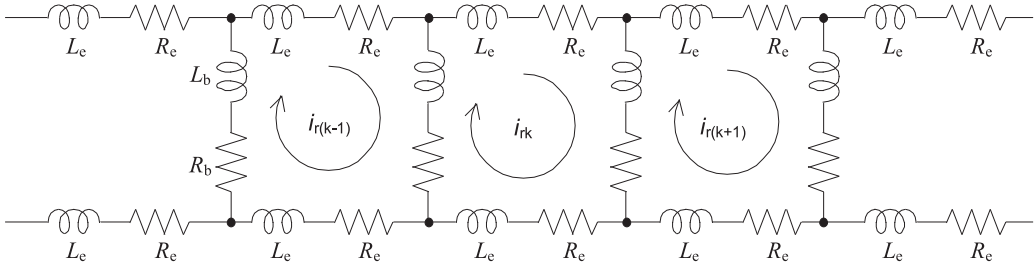

Fig. 1. Rotor loops in induction motor.

3 ELECTRICAL EQUATIONS

Consider a squirrel cage induction machine having three identical and symmetrical phases in the stator. The rotor cage having $(N_r = n)$ bars is viewed as n identical spaced loops and the currents distribution can be specified in terms of $n+1$ independent rotor currents. These currents are formed of n rotor loop currents $[i_{nr}]$ plus a circulating current in one of the end rings i_e (Figure 1). The mesh model is based on a coupled magnetic circuits approach and by making the following assumptions:

- The state of operation remains far from magnetic saturation.
- The magnetic permeability of iron is considered to be infinite and the air-gap is very small and smooth.

The stator voltage equations in vector matrix form can be written as:

$$[V_{3s}] = [R_s][i_{3s}] + \frac{\mathrm{d}}{\mathrm{d}t}[\psi_{3s}]\,, \tag{4}$$

$$\begin{bmatrix} [V_r] \\ V_e \end{bmatrix} = [0] = \begin{bmatrix} [R_r] & R_e/n \\ & \vdots \\ R_e/n \;\cdots & R_e \end{bmatrix} \cdot \begin{bmatrix} [i_{rn}] \\ i_e \end{bmatrix} + \frac{d}{dt}\begin{bmatrix} \psi_{rn} \\ \psi_e \end{bmatrix} \tag{5}$$

$$[\psi_{3s}] = [L_s][i_{3s}] + [M_{sr}][i_{nr}] \tag{6}$$

$$\begin{bmatrix} [\psi_{nr}] \\ \psi_e \end{bmatrix} = \begin{bmatrix} [M_{rs}] \cdot [i_{3s}] \\ 0 \end{bmatrix} + \begin{bmatrix} [L_r] & L_e/n \\ & \vdots \\ L_e/n \;\cdots & L_e \end{bmatrix} \cdot \begin{bmatrix} [i_{rn}] \\ i_e \end{bmatrix} \tag{7}$$

As usual, $[V]$ is the voltage matrix, $[i]$ is the current matrix. $[R_s]$ and $[R_r]$ are the stator and rotor resistance matrixes respectively, $[\Psi_s]$ and $[\Psi_r]$ are the stator and rotor flux linkage matrixes respectively. and are the stator and rotor matrixes of inductances respectively. $[M_{sr}]$ is the mutual matrix inductances between the stator and rotor, $[M_{rs}]$ is the transpose of $[M_{sr}]$. further

$$[i_{rn}] = [\, i_{r1} \quad i_{r2} \quad \cdots \quad i_{rn} \,]^T \tag{8}$$

$$[V_{3s}] = [\, V_{s1} \quad V_{s2} \quad V_{s3} \,]^T \tag{9}$$

$$[i_{3s}] = [\, i_{s1} \quad i_{s2} \quad i_{s3} \,]^T \tag{10}$$

$$[R_s] = R_s \cdot 1_{3x3} \tag{11}$$

The matrix $[R_r]$ is n by n symmetric where, $R_{b,k-1}$ is resistance of the bar number k and R_e is the end ring segment resistance.

$$[R_r] = \begin{bmatrix} R_{b0} + R_{b(N_r-1)} + 2\frac{R_e}{N_r} \cdots & 0 & 0 & \cdots \\ \vdots & \vdots & \vdots & \\ 0 \quad \cdots & -R_{b(k-1)} & R_{bk} + R_{b(k-1)} + 2\frac{R_e}{N_r} & \cdots \\ \vdots & \vdots & \vdots & \\ -R_{b(N_r-1)} \quad \cdots & 0 & 0 & \cdots \end{bmatrix} \tag{12}$$

4 CALCULATIONS OF INDUCTANCES

The inductances of the above system of equations were calculated using the winding function method, from which inductance between any two windings "i" and "j" in any electric machine can be computed by the following equation [1, 3, 4]:

$$L_{ij}(\varphi) = \mu_o L\, r \int_0^{2\pi} \frac{n_i(\varphi,\theta)\, N_j(\varphi,\theta)}{e(\varphi,\theta)} d\theta \tag{13}$$

where: φ is the angular position of the rotor with respect to some stator reference, θ is a particular angular position along the stator inner surface, e is the air gap function, L is the length of stack and r is the average radius of air gap. Further on, $n_i(\varphi,\theta)$ is the winding distribution of coil i; it was introduced to describe the considered coil, and $N_i(\varphi,\theta)$ is the winding function of coil j; it represents the mmf of the air-gap produced by unit current flowing in the considered coil.

The motor used for simulation in this paper is a three phase, 50 Hz, 2 poles, 36 stator slots and 28 rotor bars. The mutual inductances between stator and rotor are considered to be time-varying, the others inductances are pre-calculated and treated as constant because of the round stator and rotor structure.

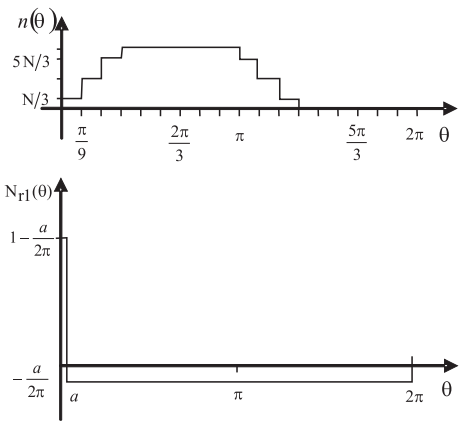

Fig. 2. Winding distribution of stator phase a (top), Winding function of rotor loop 1 (bottom)e

Figure 2 shows the turn function or the mmf distribution of the stator phase "sa" and the winding function of the rotor loop 1.

Table 1 gives the mutual inductances M_{sar1} between phase "sa" of the stator winding and the first rotor loop "r1". The mutual inductance of the stator phase "sb" and the rotor loop 1 " M_{sbr1} " is the same given by Table 1 but shifted to the right by $2\pi/3$, and that of the stator phase "sc" and the rotor loop 1 " M_{scr1} " is shifted to the left by $2\pi/3$, Figure 3.

Mutual inductances between phase "sa" and rotor loops, 2, 3, 4,*dots* is the same as given by Table 1, but shifted to the left by $a, 2a, 3a, \ldots$ respectively, Figure 4. Where $a = p\frac{2\pi}{N_r}$ is the electrical angle of a rotor loop.

The $[L_r]$ is n by n symmetrical matrix, where L_b is the rotor leakage inductance, the rotor end ring leakage inductance and L_e is the mutual inductance. All inductances are derived using (13).

$$[L_r] = \begin{bmatrix} L_{rp} + 2L_b + 2\frac{L_e}{N_r} & \ldots & M_{rr} & M_{rr} & \ldots \\ \vdots & & \vdots & \vdots & \\ M_{rr} & & M_{rr} - L_b & L_{rp} + 2L_b + 2\frac{L_e}{N_r} & M_{rr} - L_b & \ldots \\ \vdots & & \vdots & \vdots & \\ M_{rr} - L_b & \ldots & M_{rr} & M_{rr} & M_{rr} & \ldots \end{bmatrix} \tag{14}$$

The space distribution of the mutual inductance is not sinusoidal. This implies that the mutual inductances matrix presents harmonics with respect to the electrical angle θ. Consequently, this matrix can be resolved into its Fourier series [12]:

$$[M_{sr}] = \sum_{h=1}^{\infty} M_{srh} \begin{bmatrix} \ldots & \cos\big(h(\theta + \varphi_h + ka)\big) & \ldots \\ \ldots & \cos\big(h(\theta + \varphi_h + ka) - \frac{2\xi_h \pi}{3}\big) & \ldots \\ \ldots & \cos\big(h(\theta + \varphi_h + ka) + \frac{2\xi_h \pi}{3}\big) & \ldots \end{bmatrix} \tag{15}$$

where ξ_h is the initial phase angle, and $k = 0, 1, 2, \ldots, N_r$ and

$$\xi_h = \begin{cases} +1 & \text{if } h \in F \\ -1 & \text{if } h \in B \end{cases}$$

and $F = \{1, 7, 13, 19, \ldots\}$, set of forward harmonic components, and $B = \{5, 11, 17, \ldots\}$ set of backward harmonic components.

Table 1. Mutual inductance between the stator phase a and the first rotor loop

Inductance M_{sar1} (H)	Angle θ (rad)
$\frac{\mu_0 r l N_S}{g}\left(-\frac{2}{3}a\right)$	$0 \leqslant \theta < \frac{\pi}{9} - a$
$\frac{\mu_0 r l N_S}{g}\frac{2}{3}\left(\theta - \frac{\pi}{9}\right)$	$\frac{\pi}{9} - a \leqslant \theta < \frac{\pi}{9}$
0	$\frac{\pi}{9} \leqslant \theta < \frac{2\pi}{9} - a$
$\frac{\mu_0 r l N_S}{g}\frac{2}{3}\left(\theta + a - \frac{2\pi}{9}\right)$	$\frac{2\pi}{9} - a \leqslant \theta < \frac{2\pi}{9}$
$\frac{\mu_0 r l N_S}{g}\frac{2}{3}a$	$\frac{2\pi}{9} \leqslant \theta < \frac{\pi}{3} - a$
$\frac{\mu_0 r l N_S}{g}\left(\frac{\theta}{3} + a - \frac{\pi}{9}\right)$	$\frac{\pi}{3} - a \leqslant \theta < \frac{\pi}{3}$
$\frac{\mu_0 r l N_S}{g}a$	$\frac{\pi}{3} \leqslant \theta < \pi - a$
$\frac{\mu_0 r l N_S}{g}\left(-\frac{\theta}{3} + \frac{2}{3}a + \frac{\pi}{3}\right)$	$\pi - a \leqslant \theta < \pi$

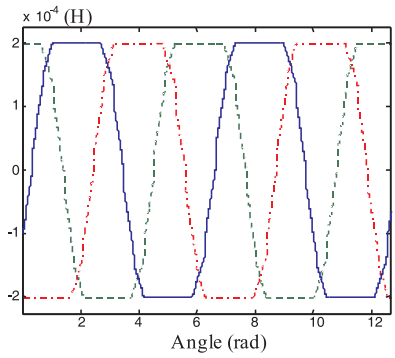

Fig. 3. Mutual inductance M_{sar1}, M_{sbr1}, M_{scr1}

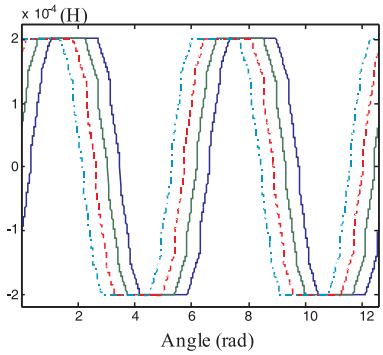

Fig. 4. Mutual inductance M_{sar1}, M_{sar2}, M_{sar3}, M_{sar4}

5 PARK TRANSFORMATION

The Park transformation is a well-known three-phase to two-phase transformation in machine analysis. The transformation equation is of the form:

$$[X_{sodq}] = [\,X_{so} \quad X_{sd} \quad X_{sq}\,]^{\top} = [P_3(\theta_s)]^{\top}[X_{3s}]\,, \quad (16)$$

where the adq transformation matrix is defined as

$$[P_3(\theta_s)] = \sqrt{\frac{2}{3}}\begin{pmatrix} 1/\sqrt{2} & \cos(\theta_s) & -\sin(\theta_s) \\ 1/\sqrt{2} & \cos(\theta_s - 2\pi/3) & -\sin(\theta_s - 2\pi/3) \\ 1/\sqrt{2} & \cos(\theta_s + 2\pi/3) & -\sin(\theta_s + 2\pi/3) \end{pmatrix}. \quad (17)$$

Here θ_s is the angular displacement between the Park reference and the first phase of the stator.

Transforming the above sets of stator abc variables to the Park reference frame using (11), we obtain

$$[V_{sodq}] = [R_s][i_{sodq}] + \frac{\mathrm{d}}{\mathrm{d}t}\big([\psi_{sodq}]\big) + \frac{\mathrm{d}\theta_s}{\mathrm{d}t}\begin{pmatrix} 0 & 0 & 0 \\ 0 & 0 & -1 \\ 0 & 1 & 0 \end{pmatrix}[\psi_{sodq}] \quad (18)$$

$$\begin{bmatrix} [V_r] \\ V_e \end{bmatrix} = [0] = \begin{bmatrix} [R_r] & R_e/n \\ & \vdots \\ R_e/n \;\cdots & R_e \end{bmatrix} \cdot \begin{bmatrix} [i_{rn}] \\ i_e \end{bmatrix} + \frac{d}{dt}\begin{bmatrix} \psi_{rn} \\ \psi_e \end{bmatrix} \quad (19)$$

$$[\psi_{sodq}] = [L_{sc}] \cdot [i_{sodq}] + [M_{srp}] \cdot [i_{nr}] \quad (20)$$

$$[\psi_{nr}] = [M_{srp}]^{t} \cdot [i_{sodq}] + [L_r] \cdot [i_{rn}] + \frac{L_e}{n} \cdot \begin{bmatrix} 1 \\ \vdots \\ 1 \end{bmatrix} \cdot [i_e] \quad (21)$$

where

$$[L_{sc}] = [P_3(\theta_s)]^{-1} \cdot [L_s] \cdot [P_{3s}(\theta_s)] = \begin{bmatrix} L_{so} & 0 & 0 \\ 0 & L_{sc} & 0 \\ 0 & 0 & L_{sc} \end{bmatrix} \quad (22)$$

where L_{so}, L_{sc} are the cyclic stator inductances.

$$[M_{srp}] = [P_3(\theta_s)]^{-1}[M_{sr}] = \sqrt{\frac{3}{2}}\sum_{h=1}^{\infty} M_{srh} \times \begin{bmatrix} \dots & 0 & \dots \\ \dots & \cos\big(\theta_s - h\xi_h(\theta + \varphi_h + ka)\big) & \dots \\ \dots & -\sin\big(\theta_s - h\xi_h(\theta + \varphi_h + ka)\big) & \dots \end{bmatrix} \quad (23)$$

From (20) and (21) we obtain:

$$\frac{d\,[\psi_{sodq}]}{dt} = [L_{sc}] \cdot \frac{d\,[i_{sodq}]}{dt} + [M_{srp}] \cdot \frac{d\,[i_{nr}]}{dt} + \frac{d\theta}{dt}\frac{d\,[M_{srp}]}{d\theta} \cdot [i_{nr}] \quad (24)$$

$$\frac{d\,[\psi_{nr}]}{dt} = [M_{srp}]^{t} \cdot \frac{d\,[i_{sodq}]}{dt} + \frac{d\theta}{dt}\frac{d\,[M_{srp}]^{t}}{d\theta} \cdot [i_{sodq}] + [L_r] \cdot \frac{d\,[i_{rn}]}{dt} + \frac{L_e}{n} \cdot \begin{bmatrix} 1 \\ \vdots \\ 1 \end{bmatrix} \cdot \frac{d\,[i_e]}{dt} \quad (25)$$

The relation between θ_s and θ is

$$\theta_s = \theta_r + \theta\,, \quad (26)$$

where θ_r is the angular displacement between the Park reference frame and the first rotor loop.

The derivative of $[M_{srp}]$ is obtained in a simple manner, for example in the case of a fixed Park frame on the rotor $(\theta_r = 0)$ it is given by

$$\frac{\mathrm{d}[M_{srp}]}{\mathrm{d}\theta} = \sqrt{\frac{3}{2}}\sum_{h=1}^{\infty} M_{srh}(h - \xi_h) \times \begin{bmatrix} \dots & 0 & \dots \\ \dots & -\sin\big((h - \xi_h)\theta + h\varphi_h + hka\big) & \dots \\ \dots & \xi_h \cos\big((h - \xi_h)\theta + h\varphi_h + hka\big) & \dots \end{bmatrix}. \quad (27)$$

For the purpose of digital simulation equations (18) and (19) are presented in state variable form with currents as state variables

$$[L]\frac{\mathrm{d}}{\mathrm{d}t}[I] = [V] - [R][I]\,, \quad (28)$$

where

$$[I] = \begin{bmatrix} [i_{sodq}] \\ [i_{rn}]_{n\times 1} \\ i_e \end{bmatrix}, \quad [V] = \begin{bmatrix} [\nu_{sodq}] \\ [V_{rn}] = [0]_{n\times 1} \\ V_e = 0 \end{bmatrix}, \quad (29)$$

$$[L] = \begin{bmatrix} [L_{sc}] & [M_{srp}] & [0]_{3\times 1} \\ [M_{srp}]^{\top} & [L_r] & \left[\frac{L_e}{n}\right]_{n\times 1} \\ [0]_{1\times 3} & \left[\frac{L_e}{n}\right]_{1\times n} & L_e \end{bmatrix}, \quad (30)$$

$$[R] = \begin{bmatrix} [R_s] + \frac{\mathrm{d}\theta_s}{\mathrm{d}t}[J_{22}][L_{sc}] & \frac{\mathrm{d}\theta}{\mathrm{d}t}\frac{\mathrm{d}[M_{srp}]}{\mathrm{d}\theta} + \frac{\mathrm{d}\theta_s}{\mathrm{d}t}[J_{22}][M_{srp}] & [0]_{3\times 1} \\ \frac{\mathrm{d}\theta}{\mathrm{d}t}\frac{\mathrm{d}[M_{srp}]^{\top}}{\mathrm{d}\theta} & [R]_r & \frac{\mathrm{d}\theta}{\mathrm{d}t}\frac{\mathrm{d}[M_{srp}]^{\top}}{\mathrm{d}\theta} \\ [0]_{1\times 3} & \left[\frac{R_e}{n}\right]_{1\times n} & R_e \end{bmatrix}. \quad (31)$$

6 MECHANICAL EQUATIONS

The mechanical equations can be expressed as

$$\frac{\mathrm{d}\omega}{\mathrm{d}t} = \frac{p}{J}(\Gamma_e - \Gamma_r)\,, \tag{32}$$

$$\frac{\mathrm{d}\theta}{\mathrm{d}t} = \omega \tag{33}$$

where Γ_e is the electromagnetic torque produced by the motor, Γ_r is the load torque and ω is the rotor speed.

Using the basic principle of energy conversion, the torque developed by the machine Γ_e can be obtained by considering the change in co-energy "W_{co}" of the system produced by a small change in rotor position when the currents are held constant.

$$\Gamma_e = \left[\frac{\partial W_{co}}{\partial \theta_{mec}}\right]_{(i_{3s}, j_{rn}\ const.)} \tag{34}$$

as the magnetic nonlinearity is ignored, the co-energy is given by

$$W_{co} = \frac{1}{2}\left[\,[i_{3s}]^\top \quad [i_{rn}]^\top\,\right]\begin{bmatrix}[L_s] & [M_{sr}]\\ [M_{rs}] & [L_r]\end{bmatrix}\begin{bmatrix}[i_{3s}]\\ [i_{rn}]\end{bmatrix}, \tag{35}$$

$$\Gamma_e = [i_{3s}]^\top \frac{\partial}{\partial \theta_{mec}}[M_{sr}][i_{rn}]\,, \tag{36}$$

$$\Gamma_e = p[i_{sdq}]^\top [p_3(\theta_s)]^\top \frac{\partial}{\partial \theta}[M_{sr}][i_{rn}]\,, \tag{37}$$

Substituting (15) and (17) in (37) leads to:

$$\Gamma_e = \sqrt{\frac{3}{2}}p\sum_{h=1}^{\infty}\Bigg[hM_{srh}\Bigg\{i_{qs}\sum_{k=0}^{N_r-1} I_{rk}\xi_k\cos\big(h(\theta+\varphi_h+ka)-\xi_k\theta_s\big) - i_{ds}\sum_{k=0}^{N_r-1} I_{rk}\sin\big(h(\theta+\varphi_h+ka)-\xi_k\theta_s\big)\Bigg\}\Bigg] \tag{37}$$

7 SIMULATION RESULTS

7.1 Analysis of Healthy machine

The differential equations derived above can be solved by fourth-order Runge-Kutta method. The simulation study was conducted using a machine of 3 hp, 3 phases, 50 Hz, 36 stator slots, 28 rotor bars and 2 poles machine.

For purposes of comparison the healthy machine was first modelled using the conventional Park d-q model. (Figure 5) The same machine was simulated next using the proposed model. The simulation results are carried out at a slip around 0.035 (Figure 6)

Comparison of the two simulation traces shows very good correlation. The effects of rotor slot harmonics can be observed to have a more significant affect on the electromagnetic torque.

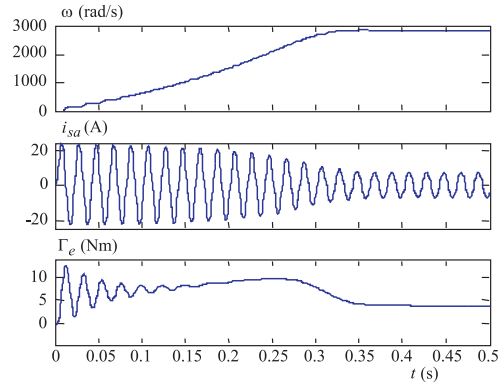

Fig. 5. Acceleration transient using conventional dq mesh model under sinusoidal voltage excitation.

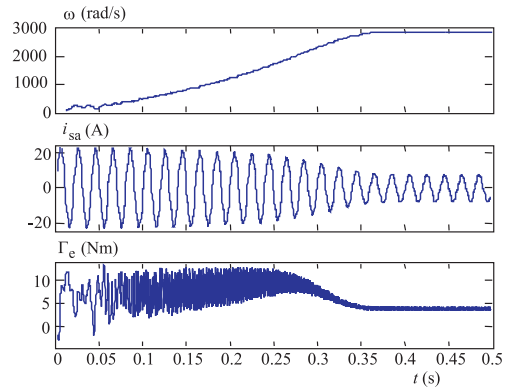

Fig. 6. Acceleration transient using the proposed model under sinusoidal voltage excitation.

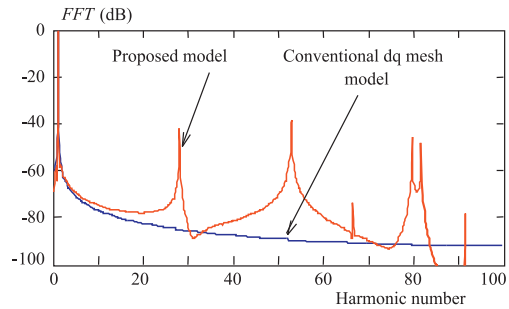

Fig. 7. Normalized FFT of the stator current in quasi steady-state. Conventional dq mesh model (blue line), proposed one (red line).

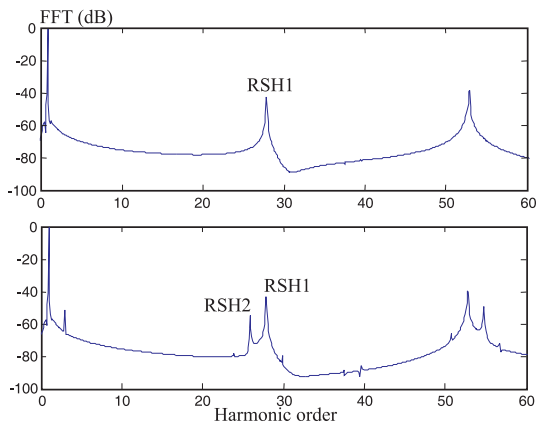

Fig. 8. Simulated, normalized FFT spectrum of machine line current of healthy induction motor with balanced supply (top) and with 5 % unbalanced supply, (bottom)

Figure 7 shows the FFT normalized to the fundamental of the line current for the conventional and the proposed d-q model. It can be easily seen the presence of the rotor slot harmonics in the case of the proposed model.

Also, we can verify the total agreement between theoretical formulas (1) and (2) and the simulations results.

For bars and , as predicted theoretically, only one RSH can be seen .The second RSH did not show up because of the pole pair number associated $\left(\frac{N_r}{p} - 1 = 27\right)$ do not belong to G (equation 2).

In order to verify that the second RSH is due to the reverse rotating field [11], five percent of unbalance was added to one of the supply phase voltages. The result is shown in Figure 8. It is clear that RSH2 can now be seen.

7.2 Analysis of machine with broken rotor bars

The studied machine was simulated with incipient broken bars under similar load and inertia conditions. To simulate a broken rotor bar, we increase its resistance by a coefficient such as the current in the bar is closest to zero. The results are shown in Figure 9. In this case, broken bar related harmonic components are clearly located around the fundamental (Figures 10).

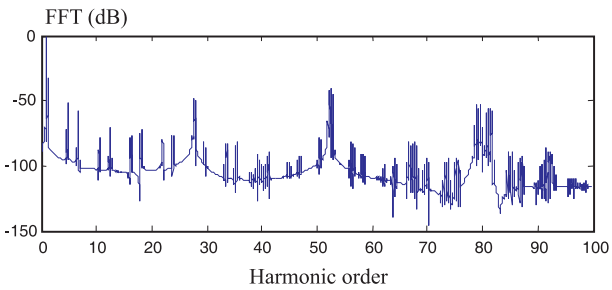

Fig. 9. Simulated, normalized line current spectra of machine with 4 broken bars

These classical twice slip frequency sidebands are not the only effect due to rotor broken bars. There are other frequencies induced around all rotor slot harmonics (Figure11).

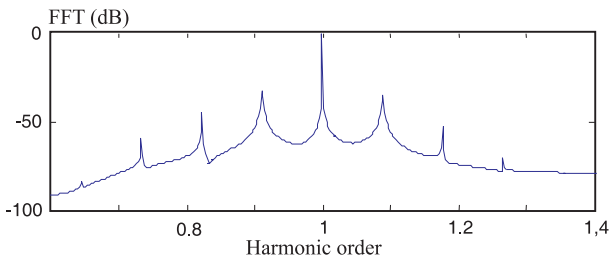

Fig. 10. Zoomed spectrum of the stator current around the fundamental

These harmonic components come from the mathematical relations given in (3), they can give additional information about the rotor asymmetry and its gravity.

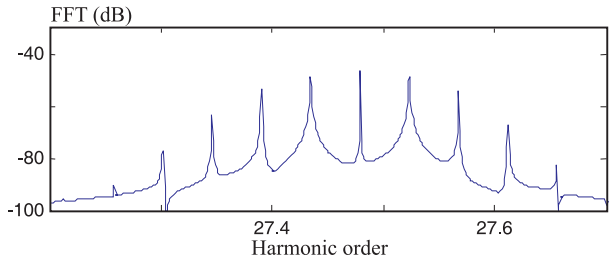

Fig. 11. Zoomed spectrum of the stator current around the around the first RSH

8 CONCLUSION

An accurate transient model of squirrel cage induction machine has been presented. This model is based on multiple coupled circuits and takes into account the geometry and winding layout of the machine, without complexity in equations formulation or long computation.

Model equations are directly extracted by the decomposition into Fourier series of the mutual inductance matrix and the presentation of the induction motor in dq frame. This model is helpful in quantifying the rotor slot harmonics under healthy as well as faulty condition. It has been shown that:

- The reverse rotating field caused by the supply unbalance induce some of space harmonics in the stator current.
- For machines with broken rotor bars, the stator current spectrum contains other significant harmonic components than $(1 \pm 2ks)\, f_s$. These harmonics can be located around all RSH.

9 APPENDIX

V	rated voltage	220 V
p	number of pole pairs	1
f_s	supply frequency	50 Hz
N_r	number of rotor bars	28
e	air gap length	0.003 m
J	inertia momentum	4.5×10^{-3} kg m^2
L_b	rotor bar leakage	0.1 mH
R_s	stator resistance	9.2 Ω
R_b	rotor bar resistance	$68 \times 10^{-6}\Omega$
R_e	end ring resistance	1.3×10^{-6}
L_{rp}	rotor loop self inductance	0.17×10^{-6} H
L_e	rotor end ring leakage inductance	2×10^{-9} H

References

[1] XIAOGANG LUO—YUEFENG LIAO—TOLIYAT, H. A.—El-ANTABLY, A.—LIPO, T. A.: IEEE Transactions on Industry Applications **31** No. 2 (March-April 1995), 311–318.

[2] MUNOZ, A. R.—LIPO, T. A.: Complex Vector Model of the Squirrel-Cage Induction Machine Including Instantaneous Rotor Bar Currents, IEEE Transactions on Industry Applications **35** No. 6 (November-December 1999), 1332–1340.

[3] JOKSIMOVIC, G. M—PENMAN, J.: The Detection of Inter-turn Short-circuits in the Stator Windings of Operating Motors, IEEE Transactions on Industrial Electronics **47** No. 5 (October 2000), 1078–1084.

[4] DEVANNEAUX, V.—DAGUES, B.—FAUCHER, J.—BARAKAT, G.: An Accurate Model of Squirrel Cage Induction Machines under Stator Faults, Mathematics and Computers in Simulation **63** (2003), 377–391.

[5] GULDMIR, H.: Detection of Airgap Eccentricity Using Line Current Spectrum of Induction Motors, Electric Power Systems Research **64** (2003), 109–117.

[6] NANDI, S.—AHMED, S.—TOLIYAT, H. A.—BHARADWAJ, R. M.: Detection of Rotor Slot and Other Eccentricity Related Harmonics in a Three Phase Induction Motor with Different Rotor Cages, IEEE Transactions on Energy Conversion **16** No. 3 (September 2001), 253–260.

[7] FERRAH A.– HOGBEN-LAING P. J.– BRADLEY K. J.– ASHER G. M.– WOOLFSON M. S.: The Effect of Rotor Design on Sensorless Speed Estimation Using Rotor Slot Harmonics Identified by Adaptive Digital Filtering Using the Maximum Likelihood Approach, IAS '97. Industry Applications Conference, 1997, **1,** (5-9 October 1997), 128–135.

[8] ALLER, J. M.—RESTREPO, J. A.—BUENO, A.—GIMENEZ, M. I.—G. PESSE: Squirrel Cage Induction Machine Model for the Analysis of Sensorless Speed Measurement Methods, Devices, Circuits and Systems, 1998, Proceedings of the Second IEEE International Caracas Conference, (2-4 March 1998).

[9] NANDI, S.—AHMED, S.—TOLIYAT, H. A.—BHARADWAJ, R. M.: Selection Criteria of Induction Machines for Speed-Sensorless Drive Applications, IEEE Transactions on Industry Applications **39** No. 3 (May-June 2003), 704–707.

[10] NANDI, S.: Modelling of Induction Machines Including Stator and Rotor Slot Effects, Industry Applications Conference, 2003. 38th IAS Annual Meeting. **2** (12–16 October 2003), 1082–1089.

[11] THOMSON, W. T.– DEANS, N. D.– LEONARD, R. A.– MILNE, A. J.: Monitoring Strategy for Discriminating Between Different Types of Defects in Induction Motors, 18-th Universities Power Engineering, Conference Proc., University of Surrey, England, 12 April 1983.

[12] CHENY, C.—KAUFFMANN, J. M.: Information Losses in Decoupling Space Harmonics Effects for an Induction Drive, Mathematics and Computers in Simulation **46** (1998), 361–372.

Received 14 April 2005

Abdelmalek Khezzar (Ing, PhD), born in 1969, received the BSc degree in electrical engineering in 1993 from Batna university — Algeria, and the PhD degree from INPL "Institut National Polytechnique de Lorraine" Nancy — France in 1997. He is currently a lecturer at Mentouri University — Constantine, Algeria, in the Department of Electrical Engineering. His main research interests are power electronics and drives and analysis of electrical machine with special emphasis on fault diagnosis.

Mohamed Yazid Kaikaa was born in Oran, Algeria, in 1977. He received the BSc degree in electrical engineering, from the University of Constantine, Algeria, in 2002, and the MSc degree in electrical and computer engineering from the Electrical Engineering Institute of Constantine University, Algeria, in 2005. He is a member of the Research Laboratory of electric machines and drives control and diagnosis of Constantine, Algeria. He is currently working on his PhD thesis.

Mohamed Boucherma was born in Jijel, Algeria, in 1959. He received the BSc degree in electrical engineering, from the University of Annaba, Algeria, in 1985, the MSc degree in power system engineering from the University of Strathclyde, Scotland, in 1989, and the PhD in electrical engineering from Sheffield University, England, in 1994. He is currently a lecturer at Mentouri University of Constantine, Algeria, in the Department of Electrical Engineering. His main research interests are power system and electrical machines.